Fluctuations of a defect line of molecular orientation in a monolayer

S. Rivière, S. Hénon, and J. Meunier
Laboratoire de Physique Statistique de l'Ecole Normale Supérieure, 24 rue Lhomond, 75231 Paris Cedex 05, France
(Received 7 June 1993)

Microscopy at the Brewster angle is used to study the phase transition that occurs during the formation of an adsorbed sodium myristate film at the surface of an aqueous solution. The formation and evolution of structures in which the tilt of the molecules creates an observable optical anisotropy are studied. Structures consisting of curved stripes of a given width are observed. Across each stripe the tilt direction of the molecules turns continuously in the plane by about 95°; two neighboring stripes are separated by curved defect lines, across which the tilt direction jumps back by about 95°. The position of these defect lines fluctuates, indicating a very low line tension. Under strong repulsions between domains, these defect lines are strongly distorted. This stripe structure can be explained by a continuum elastic model for "locked tilted mesophases," and two constants of the model can be estimated from our data.

PACS number(s): 61.30.−v, 64.70.−p, 68.10.−m, 68.15.+e

I. INTRODUCTION

During the past decade it has become more and more clear that the films of amphiphilic molecules adsorbed at the free surface of water display complicated polymorphism. It has recently become possible to determine the microscopic structure of these different phases by x-ray diffraction experiments [1]. In particular the so-called "liquid-expanded" phase is a bidimensional liquid and the so-called "liquid-condensed" phases were shown to be "locked mesophases," i.e., phases with long-range orientational (but not positional) order, in which the molecules are tilted with a fixed direction with respect to the intermolecular directions. Meanwhile, fluorescence microscopy and more recently microscopy at the Brewster [2] angle have allowed the visualization of phase coexistence and of the morphology of the denser phases. Long-range order of the direction of the molecules in the liquid-condensed phases has thus been demonstrated, and several types of defects of the molecules orientation have been observed [3–7].

We describe here the observation by microscopy at the Brewster angle of a phase transition in the film adsorbed at the free surface of an aqueous sodium myristate solution. Our observations clearly show the morphology of the dense phase domains. Furthermore, preliminary experiments show that Langmuir (insoluble) films of myristic acid on water at $p\mathrm{H}=2$ have the same behavior.

II. EXPERIMENTAL SETUP AND PRODUCTS

Microscopy at the Brewster angle is a new technique for studying Langmuir films on a macroscopic scale. It takes advantage of the fact that, at the Brewster incidence and with light polarized in the plane of incidence, the reflectivity of the air-water interface is highly sensitive to the properties of any adsorbed film on the interface [2]. It allows, for example, direct visualization of phase coexistences in monolayers (two different phases have different reflectivities). In addition, analyzing the polarization of the reflected light allows us to study the optical anisotropy of the film. Significant anisotropies have been observed [8,5,6], which probably result from the tilt of the molecules from the surface normal. If the molecules are tilted, with a tilt angle t (which is supposed to be constant all over the film, referring to the structure determination [1]) and a tilt-azimuthal direction φ from the plane of incidence (see Fig. 1), the polarization of the reflected light depends on φ. Hence when an analyzer (i.e., polarizer) is placed in the path of the reflected light, with a fixed direction, the film appears more or less bright, depending on the tilt-azimuthal direction.

Experiments were carried out on aqueous solutions of sodium myristate (or tetradecanoate), at room temperature (21 °C). Sodium myristate was purchased from Aldrich Chemie (> 99% purity grade) and used without further purification. Solutions were made in ultrapure water (MilliRO-MilliQ system), in equilibrium with the atmos-

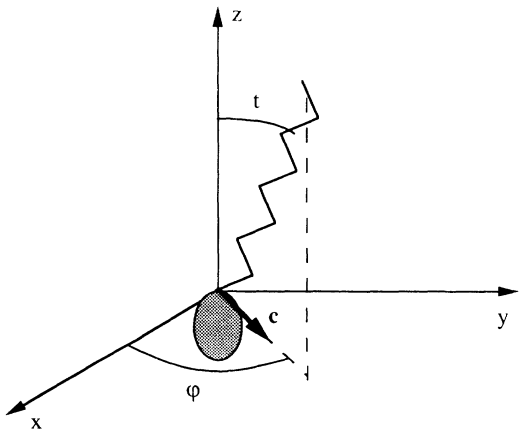

FIG. 1. Definition of the tilt angle and of the tilt-azimuthal angle. (x,z) is the plane of incidence.

pheric carbon dioxide ($p\mathrm{H} \approx 5.5$). The solubility of myristic acid in water is very low: about 20 mg/l in pure water at 20°C; thus very low concentrations were used, 4–6 mg/l, i.e., about $2.10^{-5}M$. We poured the solutions in a trough, removed any existing film by a suction device, and then followed the adsorption of the film, simultaneously by surface-tension measurements (Wilhelmy plate) and by microscopy at the Brewster angle.

In previous experiments on solutions of sodium octanoate [9], the observation of a phase transition was due to the presence of sodium hexadecanoate as an impurity [5]. This problem is avoided here, since the concentration of the solutions is low and the quantity of any impurity would be insufficient to build a monolayer.

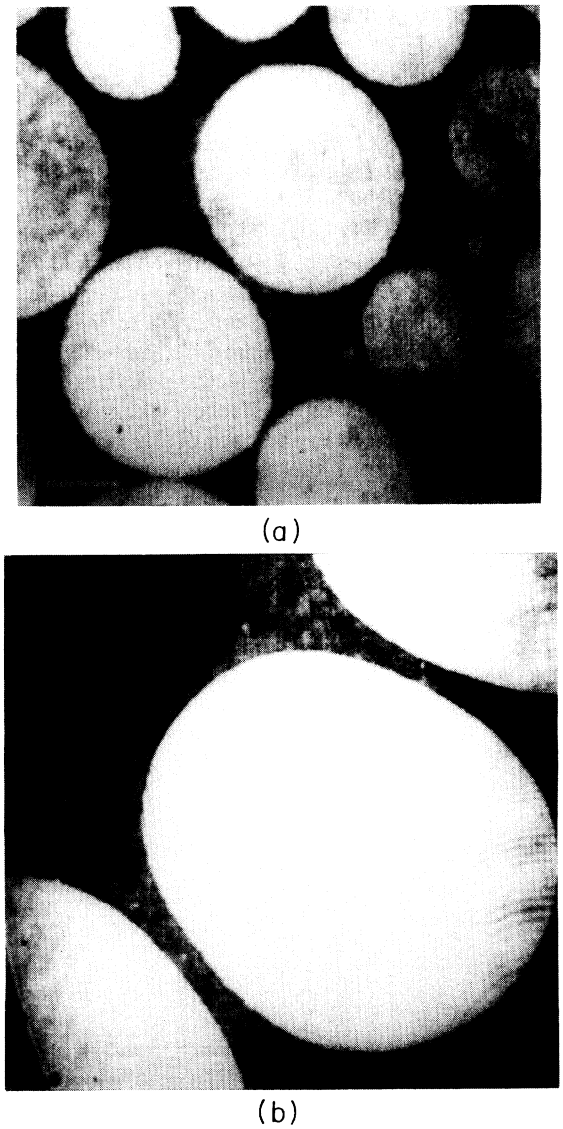

FIG. 2. Brewster-angle microscopy images: formation of the sodium myristate film, stage II. The bars represent 50 μm. Coexistence between a liquid expanded phase (dark regions) and a denser phase (bright domains) at two bulk concentrations c: (a) $c = 4$ mg/l and (b) $c = 5$ mg/l. The domains, close to each other, are strongly distorted by repulsive dipolar interactions with their neighbors.

III. FORMATION OF THE FILM

Typical Brewster-angle microscopy results for adsorbed sodium myristate films, at bulk concentrations of 4–5 mg/l, are pictured in Fig. 2. The corresponding surface pressure as a function of time for a 4-mg/l solution is plotted in Fig. 3. For solutions at 4–6 mg/l, the adsorption of the monolayer is slow (1–2 h), and several stages can be distinguished during its formation.

Stage I: First the film reflects little light and appears uniformly black. Meanwhile the surface pressure increases from a very low value to about 16 dyn/cm. This dilute phase probably corresponds to the liquid expanded state of the film.

Stage II: Ten to fifty minutes later (depending on the concentration), the surface pressure reaches a plateau, at about 16 dyn/cm, corresponding to a first-order phase transition; bright domains of a denser phase nucleate and grow to their final size within a few minutes. They are circular when far away from each other, but are strongly distorted by their neighbors when the distance between them is smaller (see Fig. 2). This distortion probably results from long-ranged dipolar interaction as suggested by Andelman, Brochard, and Joanny [10]. Domains sizes range from 150 μm^2 to more than 1 mm^2. Both the size and the size distribution of the domains are independent of the sodium myristate concentration in solution. Furthermore, for a given concentration they depend on the experiment, and for a given experiment they depend on the observed section of the surface. The size of the domains seems to depend only on the number of nucleation sites: the more numerous the domains, the smaller they are. Finally, the higher the concentration of the solution, the higher the proportion of the surface covered by the dense phase at the end of this stage, i.e., the closer the domains come to each other, as close as a few micrometers at 6 mg/l.

Stage III: Several minutes later, very small "droplets" of the liquid expanded phase appear in the dense domains (see Fig. 4), and slowly grow, from the diameter corresponding to the resolution of the microscope (about 1.5 μm) up to several tens of micrometers, until they are in contact with each other. Then they coalesce with each

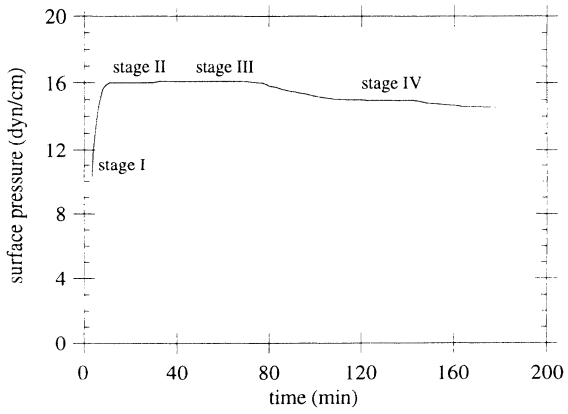

FIG. 3. Surface pressure of a sodium myristate solution at a bulk concentration $c = 4$ mg/l, as a function of time.

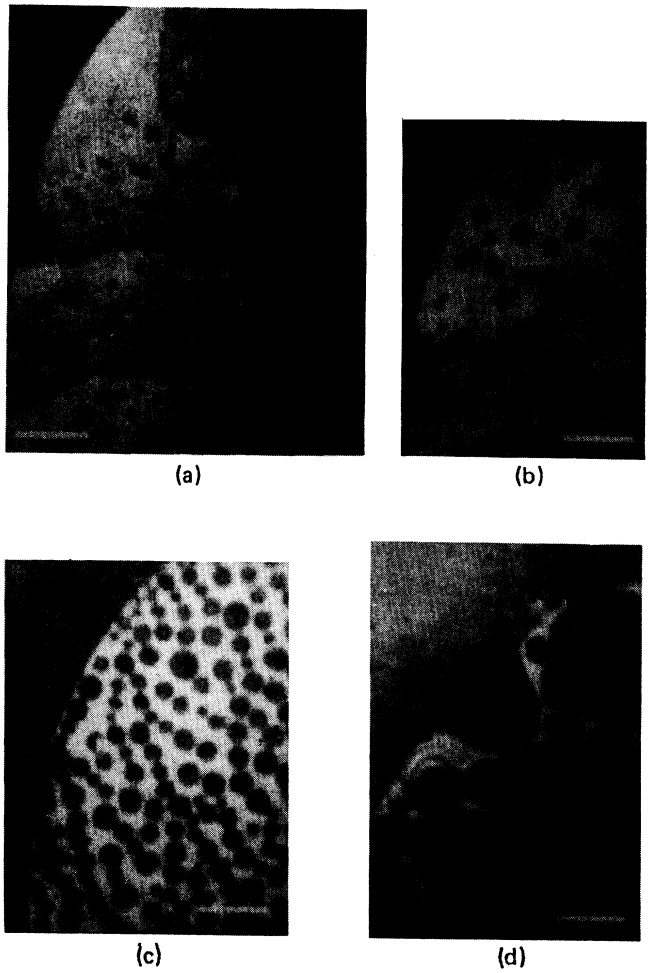

FIG. 4. Brewster-angle microscopy images: formation of the sodium myristate film, stage III. The bars represent 50 μm. The disappearance of the denser phase by the nucleation and the increase in size of droplets ("holes") of the liquid expanded phase inside the dense domains. (a) $t \sim 50$ min after the beginning of the experiment. The holes are observable for a few minutes; they are about 5 μm in diameter (the resolution of the microscope is 1.5 μm), their distribution inside the domains is not uniform, and "lines" of holes are noticeable. (b) $t \sim 75$ min. The holes are larger. (c) $t \sim 90$ min. Some holes have already coalesced with each other. (d) $t \sim 100$ min. A few seconds before the disappearance of the denser phase, a hole has just coalesced with the surrounding liquid expanded phase.

other and also coalesce with the surrounding liquid expanded phase [see Fig. 4(d)]. This phenomenon finally results in the disappearance of the dense domains. The moment the droplets appear can vary for a given concentration from one experiment to another, from less than 10 min to several tens of minutes after the nucleation of the dense phase. During this stage the surface pressure remains constant, at its plateau value. On several occasions we have observed bright three-dimensional objects on the surface. That means that the decrease of the molecular density of the film is probably due to collapse, three-dimensional crystals absorb sodium myristate, the bulk concentration of the solution decreases, and the two-dimensional dense phase melts.

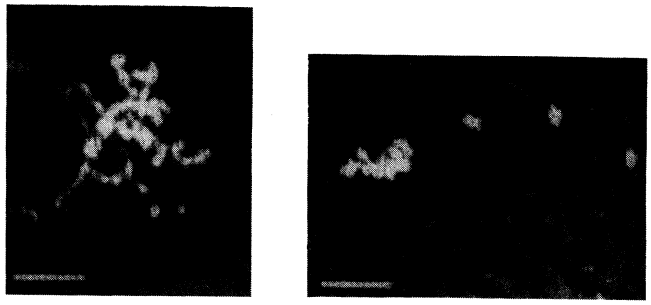

FIG. 5. Brewster-angle microscopy images, formation of the sodium myristate film, end of stage III and stage IV. The bars represent 50 μm. (a) Coexistence between the monolayer and three-dimensional objects. A few seconds before the disappearance of the denser phase, a domain (on the left) of which nothing remains except a ring around a large hole is surrounded by collapse. (b) All the domains of the denser phase have disappeared; very bright three-dimensional objects are observable, certainly collapse.

Stage IV: All the domains of the dense phase have disappeared. The film is uniformly black as in stage I, possibly with bright floating three-dimensional objects (Fig. 5). The surface pressure slowly decreases and reaches an equilibrium value, at about 14.5 dyn/cm, the equilibrium spreading pressure of this compound [11].

IV. MORPHOLOGY OF THE DENSE PHASE

A. Stripes structure

When an analyzer is placed in the path of the reflected light, an optical anisotropy is observed in the denser phase; however, the dilute phase is isotropic (confirming its liquid expanded state). This anisotropy is probably due to a tilt of the molecules from the surface normal: the dense phase is a liquid condensed [1]. Hence, as described in Sec. II, images taken with an analyzer in place display different shades of gray that correspond to different tilt-azimuthal orientations φ of the adsorbed molecules.

With a fixed orientation of the analyzer, the structure pictured in Fig. 6 is observed. The dense domains are divided by curved defect lines into parallel stripes. Within each domain, all the stripes appear to have the same width and are deformed by edge defects at the border of the domains. The width of the stripes can vary from one experiment to another and for a given experiment from one domain to another. However, the distribution of the stripe width is relatively large, ranging from 60 to 100 μm and most often centered about 75 μm, but the number of stripes observed in each experiment is too small to allow clear statistics. The mean width of the stripes increases at the very beginning of the domains growth and then remains constant. It seems to be independent of the domain size and of the concentration in solution. The number of stripes varies from 3 for the smallest domains to 12 for the largest ones (see Fig. 6).

Across each stripe the tilt-azimuthal direction turns continuously by $95° \pm 10°$. Across the defect line, separat-

ing a stripe from its next neighbor, the tilt-azimuthal direction jumps back by about 95° over a small distance, and the same structure, with the same azimuthal directions, repeats across the next neighboring stripe [6]. The width of the separating defect lines can be measured; they are seen black when having a particular direction from the analyzer axis [5], with a width of about 2 μm.

As seen in Fig. 7, the curvature of the stripes is not constant from one domain to another and it can also change along a given stripe. These curvatures are induced by the curve of the domain border. The stripes structure is not always perfect; it can be disturbed by defects (see Fig. 7). Furthermore, it can be organized around a defect point. In some large domains, six branched spirals, randomly clockwise or counterclockwise, are observed [see Fig. 7(b)]. Edge effects are also observed. Defect lines between stripes are bent on the border of the domains (see Figs. 6 and 7), and in small domains the defect point is often expelled to a small distance outside the domain (see. Fig. 6).

B. Fluctuations of the defect lines

Thermal fluctuations of the defect lines between two stripes are observed from the moment they appear. The wavelength of these fluctuations ranges from a few to a few tens of micrometers. This phenomenon can be visualized by the following image processing: the images of a line L, perpendicular to the stripes, are taken every fifteenth of a second and placed side by side to form an image (see Fig. 8). The position of the intersection of the defect lines and of the line L can thus be followed in time.

The amplitude of these fluctuations (~ 6 μm) is observed to be independent of the concentration in solution, the size of the domains (number and width of stripes), and the distance of the line to the border of the domain. However, the amplitude decreases to the point of vanishing a few minutes before the observation of visible "holes" of liquid phase inside the domains (see Sec. III, stage III). These holes are observed to be more numerous on the defect lines than anywhere else in the domains,

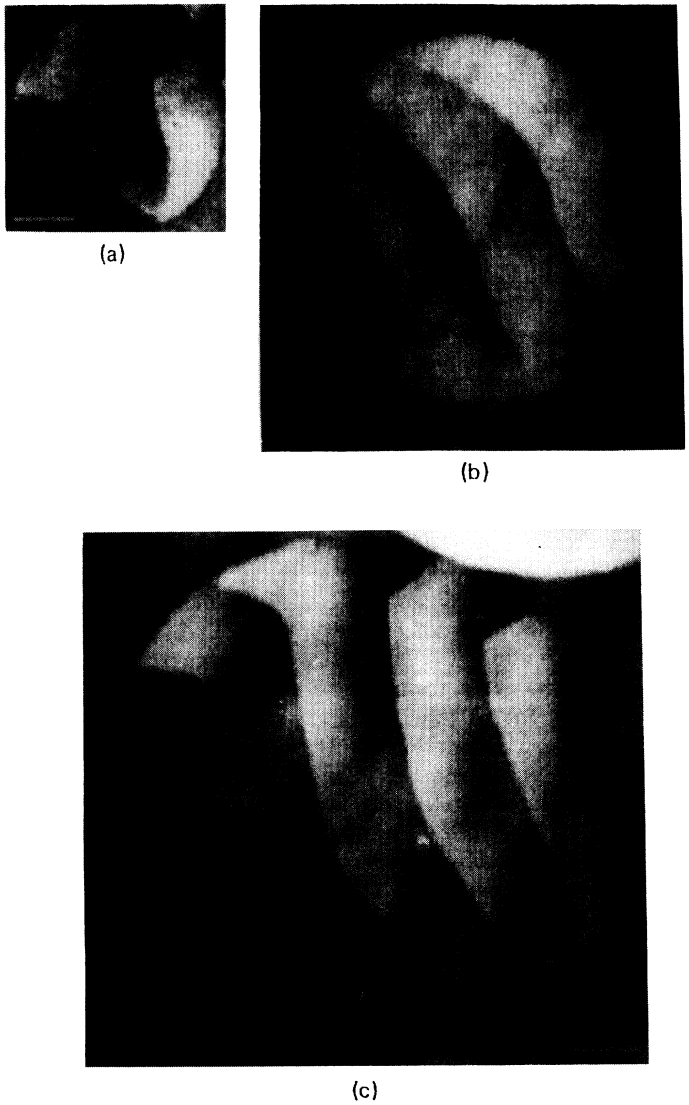

FIG. 6. Brewster-angle microscopy images with a polarizer placed in the path of the reflected light. The bars represent 50 μm. The domains in the denser phase are anisotropic and are divided into parallel strips of the same width separated by defect lines due to a sudden jump of the tilt-azimuthal direction of the molecules. Three sizes of domains are shown. Edge effects are observable on the border of the domains where the defect lines are bent. The interrupted wall in (b) (bottom center) is due to an artifact. The contrast becomes too small to appear on the picture. A direct observation shows that the wall is not interrupted.

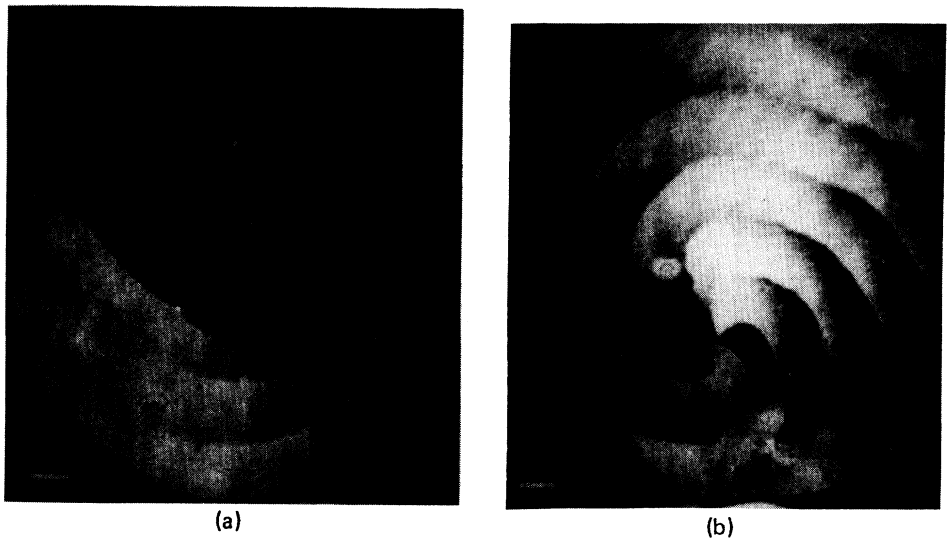

FIG. 7. Brewster-angle microscopy images with analyzer. The bars represent 50 μm. Two examples of defect points can be observed in the structure in stripes of the dense domains. The spirals are randomly clockwise or counterclockwise. In the bottom right quadrant of (b) defect lines are seen black with a width of about 2 μm.

which suggests that the vanishing of the fluctuations is due to the appearance of small (less than the resolution of the microscope) holes on the lines. This appearance of holes on the defect lines is similar to the phenomenon observed in the melting of three-dimensional crystals (i.e., melting begins at the grain boundaries).

C. Deformation of the domains and of the defect lines

When the concentration of the solution is high (about 6 mg/l), the domains come very close to each other (the distance between domains can be smaller than the resolution of the microscope) and are strongly distorted by repulsive interactions with their neighbors. Meanwhile an increase of the surface pressure, by about 2 dyn/cm, is observed (see Fig. 9), which can be explained in terms of strong dipolar interactions. The domains come sometimes so close to each other as to coalesce, despite their strong repulsion.

When the domains are strongly distorted, a deformation of the defect lines is also observed, on a scale comparable with the width of the stripes. The defect lines strongly fluctuate around their mean position, and meanwhile this mean position changes (see Fig. 10). The wavelength and amplitude of these fluctuations are about 100 μm. This phenomenon is often observed for solutions at 6 mg/l, where the domains are close, but never at 4 mg/l, where they are relatively separated. At 5 mg/l, it is sometimes observed in zones of the film where the domains are close to each other and strongly distorted, while nothing is observed on other zones of the film where the domains are not distorted. This suggests that the phenomenon is due to the strong repulsion between domains. This phenomenon disappears after 10–20 min, and the small thermal fluctuations are again observed, until a few minutes before the appearance of small holes on the lines (see Sec. II). The evolution mechanism of this deformation is not yet understood.

V. INTERPRETATION

A. Stripes structure

Very similar parallel stripes were observed in thin films of chiral liquid crystals [12,13]. A model, ignoring any underlying structure of the phase, was developed to ex-

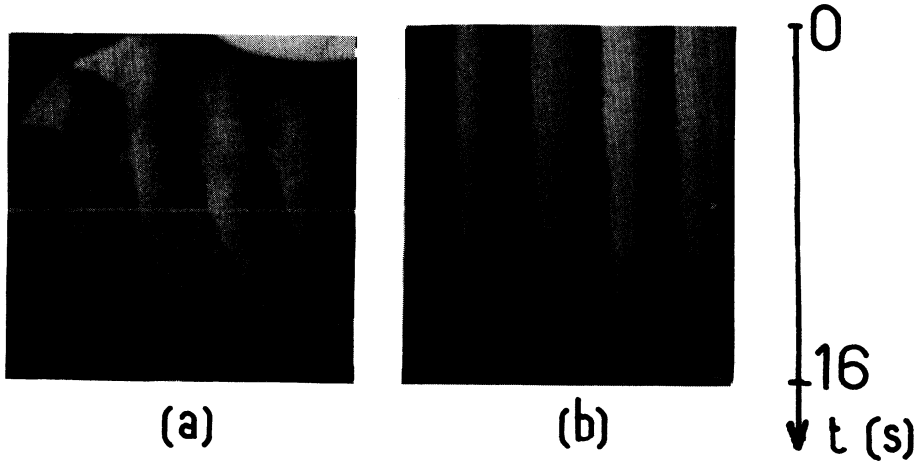

FIG. 8. Measurement of the amplitude of the thermal fluctuations of the defect lines. An image of the white line L, represented in (a), is taken every fifteenth of a second; all the images are then placed side by side. (b) The defect lines are observed to fluctuate with an amplitude of ~ 6 μm. The bars represent 10 μm.

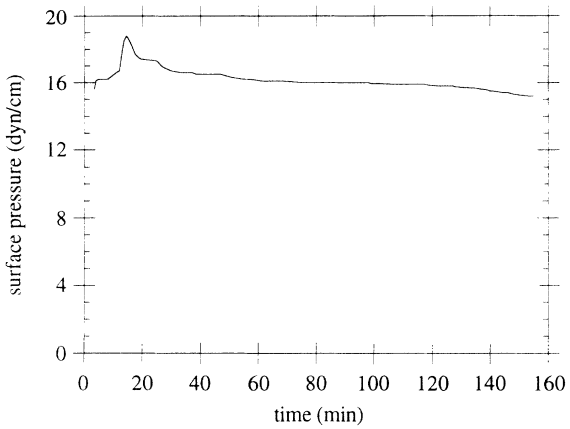

FIG. 9. Surface pressure of a sodium myristate solution at bulk concentration 6 mg/l, as a function of time. An increase by 2 dyn/cm of the surface pressure is observed during a few minutes, simultaneously with strong fluctuations of the defect lines. This phenomenon occurs when the dense domains are very distorted by strong repulsive dipolar interactions between them.

plain the appearance of that kind of stripe structure [12]. The free energy of the film is written in terms of $\mathbf{c}=\mathbf{x}\cos\varphi+\mathbf{y}\sin\varphi$, the unit vector of the molecules direction in the plane of the layer (see Fig. 1), with a spontaneous bend q and bend and splay energies K_b and K_s:

$$\mathcal{F}[\mathbf{c}]=\int\int dx\,dy F(\mathbf{c}(x;y))+\mathcal{F}_{\text{defects}}$$
$$=\int\int dx\,dy\tfrac{1}{2}\{K_s(\text{divc})^2+K_b(\text{rotc}-q)^2\}$$
$$+\mathcal{F}_{\text{defects}}\,.$$

In Langmuir films, a spontaneous bend is forbidden if the molecules are not chiral, but a spontaneous splay is possible, because of the asymmetry between the heads and the tails of the molecules. It can be modeled by assuming that the polar heads of the molecules do not have the same lateral section as the aliphatic chains. Hence the molecules are not cylindrical, but conical, as pictured in Fig. 11. In this model, defect lines with a line tension λ are supposed to exist, and a minimization of the total energy gives the correct structure. But this model is insufficient because the form of the energy does not account for the appearance of these defect lines. The underlying structure of the film has to be taken into account. The dense phase is a tilted phase and thus, as shown by x-ray diffraction experiments [1] a "tilted locked hexatic phase"; there is a long-range orientation (but not positional) order, the lattice is locally hexagonal [we will denote $\theta(x,y)$ the bond angle field which has a sixfold symmetry], and the molecules are tilted in a direction fixed with respect to the intermolecular directions (for instance, towards a nearest neighbor in the so-called L_2 phase and a next-nearest neighbor in the L_2' phase [1]). This underlying structure is taken into account in a continuum elastic model, first developed for thin films of smectic liquid crystals [13,14]. It has already been used to describe the liquid-condensed phases of Langmuir films [3,5]. The energy of the film is written as

$$F=\tfrac{1}{2}K|\nabla\varphi|^2+\tfrac{1}{2}K'|\nabla\theta|^2+g\nabla\theta\cdot\nabla\varphi+V(\theta-\varphi)\,,$$

where K and K' are elastic constants for the tilt-azimuthal and bond directions, respectively (splay and bend elasticity are supposed to be equal), g is a coupling between tilt and bond directions, and $V(\theta-\varphi)=-h_6\cos[6(\theta-\varphi)]$ is a potential locking the tilt direction to the intermolecular directions, respecting the sixfold symmetry of the structure. To describe our system, we have to add to this energy a term which favors a splay of the structure. In a model recently developed to explain the appearance of periodic stripes structures in Langmuir films of fatty acids and methyl and ethyl esters [7], Selinger [15] adds the term $\lambda_s\cos[6(\theta-\varphi)]$divc; but a spontaneous splay could be sufficient [18]. Regardless of the exact form of this term, this model predicts the appearance of defect lines, across which $\theta-\varphi$ jumps by an integral multiple of 60° (and φ by $\varphi_0\approx n[1-(K+g)/K'](\pi/3)$ rad, where n is an integer),

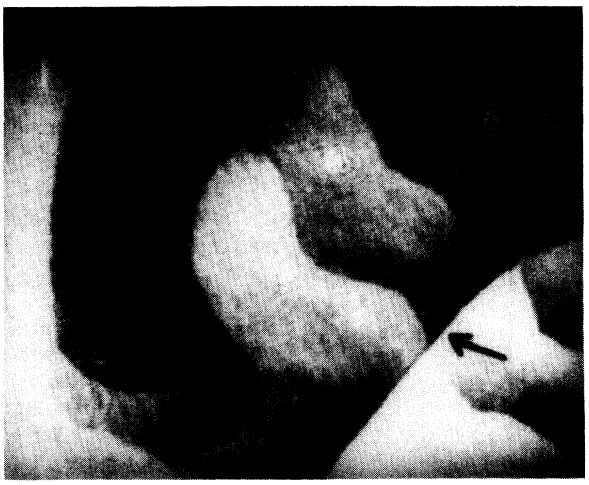

FIG. 10. Brewster-angle microscopy image with analyzer of a sodium myristate film at bulk concentration 6 mg/l. An example of the deformations of the defect lines that occur during a few minutes when the dense domains, very close to each other, are distorted by their neighbors because of strong repulsive dipolar interactions. The bar represents 50 μm. The arrows indicate the juncture between the neighboring domains.

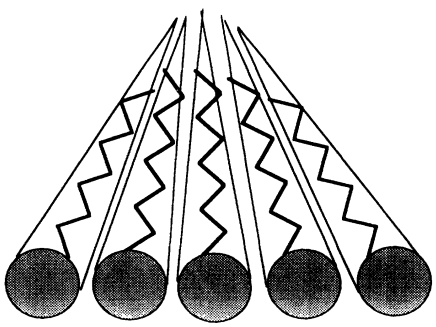

FIG. 11. Spontaneous splay for amphiphile molecules.

according the symmetry of $V(\theta-\varphi)$ [13,5]. These defect lines have an energy cost per unit length $\lambda \approx \frac{3}{4}\sqrt{K_- h_6}$ and a width $d \approx \frac{1}{6}\sqrt{K_-/h_6}$, where $K_- = (KK'-g^2)/(K+K'+2g)$. We estimated λ (see next paragraph) and it is between 10^{-14} and 10^{-13} N and d is about 2 μm. That leads to $h_6 \approx 10^{-9}-10^{-8}$ J/m^2 and $K_- \approx 10^{-19}-10^{-18}$ J (i.e., from $4k_BT$ to $40k_BT$). The huge difference between the measured azimuth jump (95°) and 60° implies a too strong coupling g between θ and φ and suggests that this model is probably insufficient to explain the experimental value of the jump.

Selinger [15] also argues that the formation of spiral structures comes from a spontaneous symmetry breaking, suggesting the existence of a chirality. As the molecules of the layer are non-chiral, the chirality must come from the underlying structure. That suggests that the liquid condensed phase observed is the so-called L_1' phase, a tilted mesophase in which the molecules are tilted in a direction intermediate between nearest neighbor and next-nearest neighbor [16;17]. However, the existence of this phase in the phase diagram of fatty acids and its precise location are not clear.

B. Fluctuations of the defect lines

The relatively high amplitude of the thermal fluctuations shows that the energy per unit length (or line tension λ) of the defect lines is low. At temperature T, the energy of thermal fluctuations at wave vector q, and with an amplitude ξ_q, of a line of length L, is

$$\varepsilon_q = \lambda(L_q - L) \approx \lambda \int_0^L dx \tfrac{1}{2} q^2 \xi_q^2 \sin^2(qx+\varphi_q) = \lambda \tfrac{1}{2} q^2 \xi_q^2 \frac{L}{2} .$$

Using the equipartition theorem $\langle \varepsilon_q \rangle = \frac{1}{2} k_B T$,

$$\langle \xi^2 \rangle = \int_{q_{\min}}^{q_{\max}} L\, dq \frac{2k_BT}{\lambda L_q^2} = \frac{2k_BT}{\lambda}\left[\frac{1}{q_{\min}} - \frac{1}{q_{\max}}\right] .$$

$q_{\max} \approx 1/d$ is a cutoff, meaning that this model does not hold on scales smaller than the width d of the defect lines; $q_{\min} \approx 1/L$, where L is the length of the line that fluctuates. The fact that the amplitude of the fluctuations is independent on the total length of the lines suggests that there are defects on the line that stop the fluctuations. L is thus not the total length of the line but the length between two defects on the line. The disappearance of the fluctuations when there are holes close to each others on the lines confirms that hypothesis. The cutoff $q_{\min}$ could also be due to a coupling between lines [18], but this explanation does not seem relevant here because the amplitude of the fluctuations is independent of the distance of the lines from the border of the domain. In our experiments, L cannot be determined exactly. It is more than 10 μm (when holes at a distance of about 10 μm are on a line, it does not fluctuate any longer) and less than about 100 μm (the length of the shorter lines to be seen fluctuating). When 10 $\mu m \le L \le 100$ μm and $\langle \xi^2 \rangle^{1/2} \sim 2$ μm, we find $10^{-14}\text{N} \lesssim \lambda \lesssim 10^{-13}$ N. This is a little higher than an estimation of the line tension from its width d,

$$\lambda \approx \frac{k_BT}{d} \approx 2\times 10^{-15} \text{ N} .$$

VI. CONCLUSION

In conclusion, we have observed a phase transition in films of sodium myristate at the free surface of its solution, between a liquid expanded and a tilted mesophase. The domains of this dense phase show orientational defects consisting of curved parallel stripes across which the molecular direction turns continuously in the plane by about 95° and separated from each other by defect lines. This structure is explained by a continuum elastic model with a spontaneous splay. The estimation of the very low line tension of the defect lines, via their thermal fluctuations, and their width allows us to estimate two of the constants in the model.

Before the end of the transition, the film collapses. This collapse consists of the slow formation of three-dimensional crystals, leading to a fusion of the dense domains in the monolayer. This melting begins by the formation of small holes in the domains, essentially along the defect lines.

ACKNOWLEDGMENTS

We are indebted to J. Prost for fruitful discussions. The Laboratoire de Physique Statistique de l'Ecole Normale Supérieure is "URA 1306 du CNRS, associées aux Universités Paris VI et Paris VII."

[1] A. M. Bibo, C. M. Knobler, and I. R. Peterson, J. Phys. Chem. **95**, 5591 (1991).

[2] S. Hénon and J. Meunier, Rev. Sci. Instrum. **62**, 936 (1991); D. Hönig and D. Möbius, J. Phys. Chem. **95**, 4590 (1991).

[3] Xia Qiu, J. Ruiz-Garcia, K. J. Stine, C. M. Knobler, and J. V. Selinger, Phys. Rev. Lett. **67**, 703 (1991).

[4] V. T. Moy, D. J. Keller, H. E. Gaub, and H. M. McConnell, J. Phys. Chem. **90**, 3198 (1986).

[5] S. Hénon and J. Meunier, J. Chem. Phys. **98**, 9148 (1993).

[6] S. Hénon and J. Meunier, Thin Solid Films **234**, 471 (1993).

[7] Xia Qiu, J. Ruiz-Garcia, and C. M. Knobler, in *Interface Dynamics and Growth*, edited by K. S. Liang, M. P. Anderson, R. F. Bruinsma, and G. Scoles, MRS Symposia Proceedings No. 237 (Materials Research Society, Pittsburgh, 1992), p. 263.

[8] D. Hönig and D. Möbius, Thin Solid Films, **210/211**, 64 (1992).

[9] S. Hénon and J. Meunier, Thin Solid Films **210/211**, 121 (1992).

[10] D. Andelman, F. Brochard, and J. F. Joanny, J. Chem. Phys. **86**, 3673 (1987).

[11] G. E. Moyd, J. Phys. Chem. **62**, 536 (1958).

[12] S. A. Langer and J. P. Sethna, Phys. Rev. A **34**, 5035 (1986).
[13] S. B. Dierker, R. Pindak, and R. B. Meyer, Phys. Rev. Lett. **56**, 1819 (1986).
[14] J. V. Selinger and D. R. Nelson, Phys. Rev. A **39**, 3135 (1989).
[15] J. V. Selinger, in *Complex Fluids,* edited by E. B. Sirota, D. Weitz, T. Wilten, and J. Israelachvili, MRS Symposia Proceedings No. 248 (Materials Research Society, Pittsburgh, 1992).
[16] A. Overbeck and D. Möbius, J. Phys. Chem. **97**, 7999 (1993).
[17] T. M. Fischer, R. Bruinsma, and C. M. Knobler (unpublished).
[18] J. Prost (private communication).

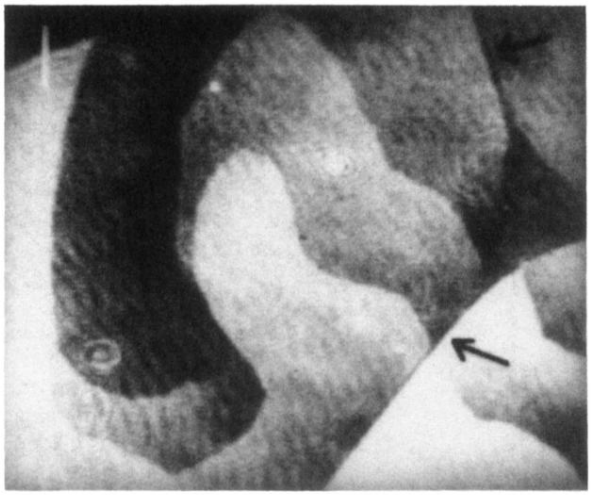

FIG. 10. Brewster-angle microscopy image with analyzer of a sodium myristate film at bulk concentration 6 mg/l. An example of the deformations of the defect lines that occur during a few minutes when the dense domains, very close to each other, are distorted by their neighbors because of strong repulsive dipolar interactions. The bar represents 50 μm. The arrows indicate the juncture between the neighboring domains.

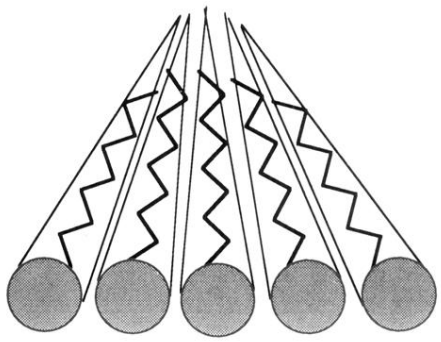

FIG. 11. Spontaneous splay for amphiphile molecules.

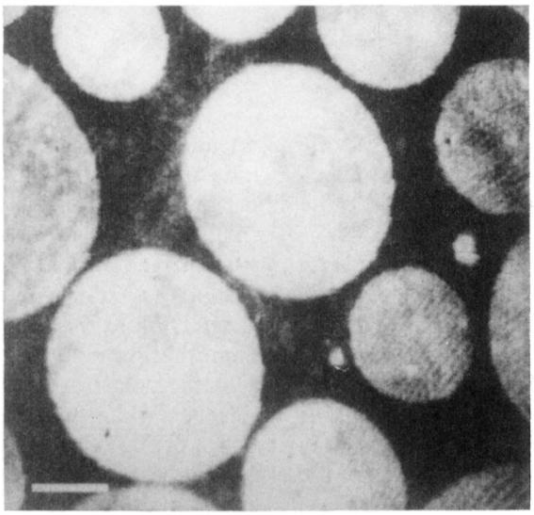

(a)

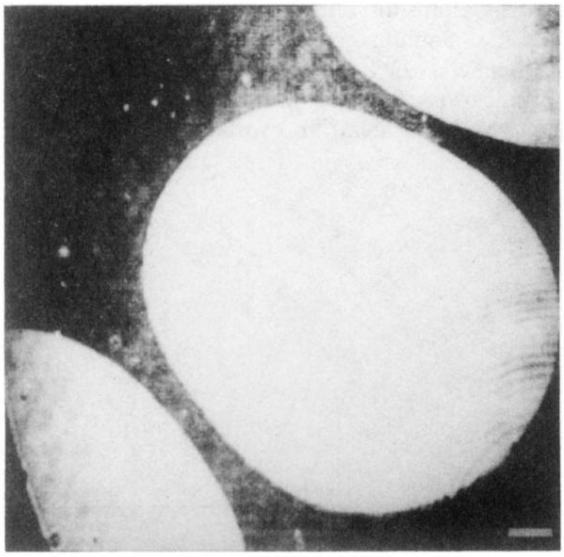

(b)

FIG. 2. Brewster-angle microscopy images: formation of the sodium myristate film, stage II. The bars represent 50 μm. Coexistence between a liquid expanded phase (dark regions) and a denser phase (bright domains) at two bulk concentrations c: (a) $c = 4$ mg/l and (b) $c = 5$ mg/l. The domains, close to each other, are strongly distorted by repulsive dipolar interactions with their neighbors.

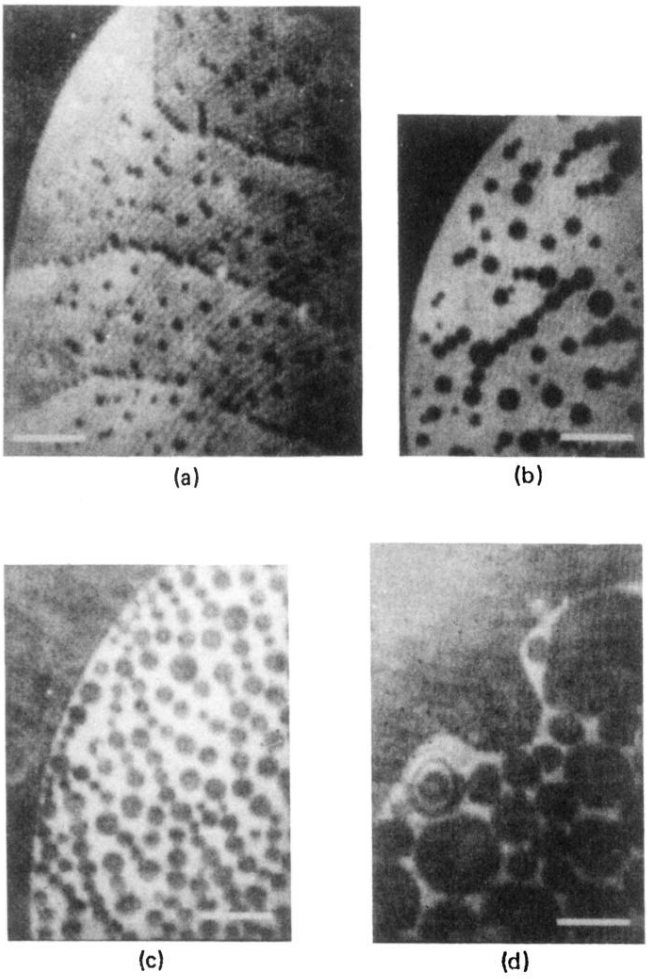

FIG. 4. Brewster-angle microscopy images: formation of the sodium myristate film, stage III. The bars represent 50 μm. The disappearance of the denser phase by the nucleation and the increase in size of droplets ("holes") of the liquid expanded phase inside the dense domains. (a) $t \sim 50$ min after the beginning of the experiment. The holes are observable for a few minutes; they are about 5 μm in diameter (the resolution of the microscope is 1.5 μm), their distribution inside the domains is not uniform, and "lines" of holes are noticeable. (b) $t \sim 75$ min. The holes are larger. (c) $t \sim 90$ min. Some holes have already coalesced with each other. (d) $t \sim 100$ min. A few seconds before the disappearance of the denser phase, a hole has just coalesced with the surrounding liquid expanded phase.

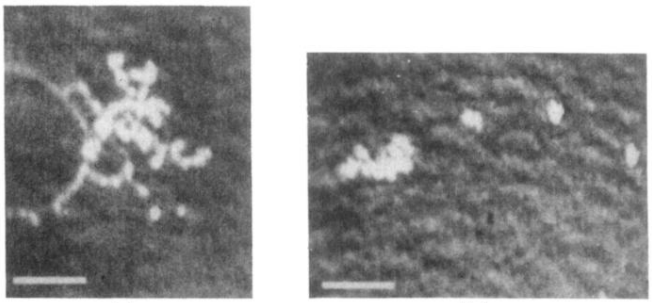

FIG. 5. Brewster-angle microscopy images, formation of the sodium myristate film, end of stage III and stage IV. The bars represent 50 μm. (a) Coexistence between the monolayer and three-dimensional objects. A few seconds before the disappearance of the denser phase, a domain (on the left) of which nothing remains except a ring around a large hole is surrounded by collapse. (b) All the domains of the denser phase have disappeared; very bright three-dimensional objects are observable, certainly collapse.

(a)

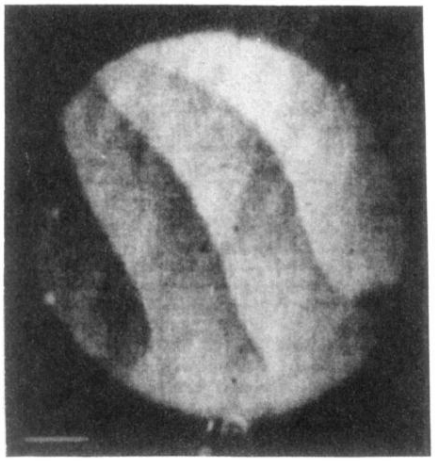

(b)

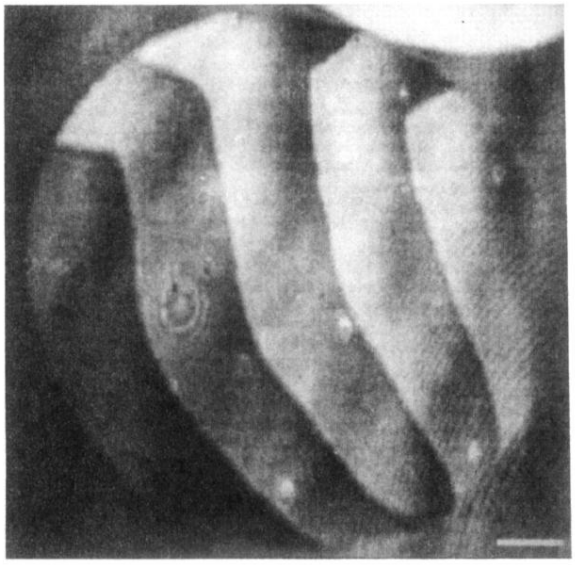

(c)

FIG. 6. Brewster-angle microscopy images with a polarizer placed in the path of the reflected light. The bars represent 50 μm. The domains in the denser phase are anisotropic and are divided into parallel strips of the same width separated by defect lines due to a sudden jump of the tilt-azimuthal direction of the molecules. Three sizes of domains are shown. Edge effects are observable on the border of the domains where the defect lines are bent. The interrupted wall in (b) (bottom center) is due to an artifact. The contrast becomes too small to appear on the picture. A direct observation shows that the wall is not interrupted.

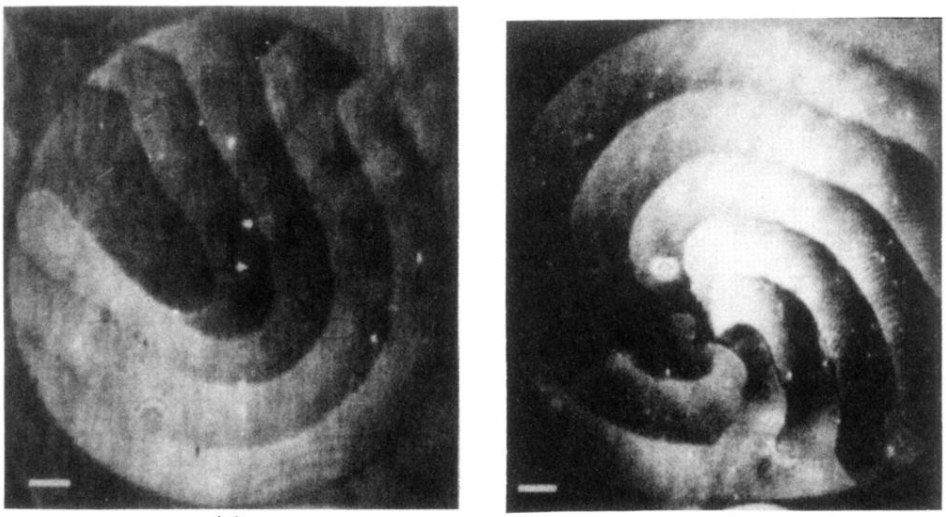

(a) (b)

FIG. 7. Brewster-angle microscopy images with analyzer. The bars represent 50 μm. Two examples of defect points can be observed in the structure in stripes of the dense domains. The spirals are randomly clockwise or counterclockwise. In the bottom right quadrant of (b) defect lines are seen black with a width of about 2 μm.

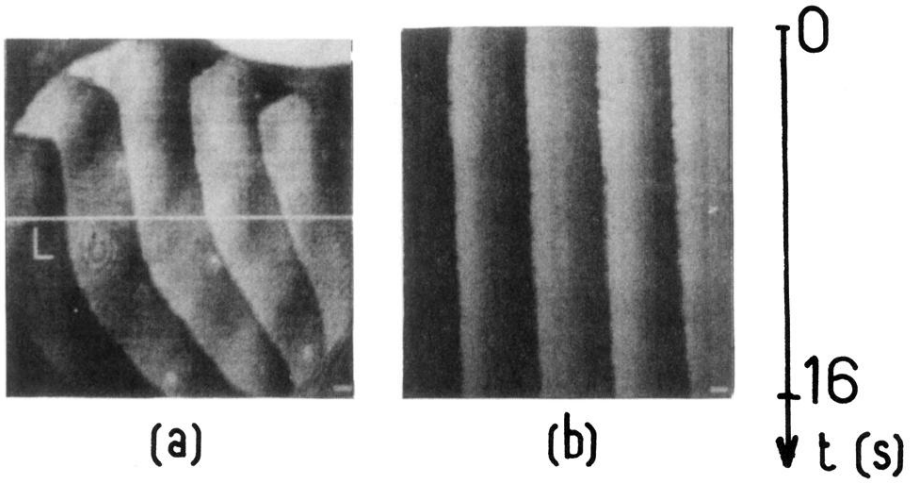

FIG. 8. Measurement of the amplitude of the thermal fluctuations of the defect lines. An image of the white line L, represented in (a), is taken every fifteenth of a second; all the images are then placed side by side. (b) The defect lines are observed to fluctuate with an amplitude of ~ 6 μm. The bars represent 10 μm.